

UNCLASSIFIED

AD 401 219

*Reproduced
by the*

DEFENSE DOCUMENTATION CENTER

FOR

SCIENTIFIC AND TECHNICAL INFORMATION

CAMERON STATION, ALEXANDRIA, VIRGINIA



UNCLASSIFIED

NOTICE: When government or other drawings, specifications or other data are used for any purpose other than in connection with a definitely related government procurement operation, the U. S. Government thereby incurs no responsibility, nor any obligation whatsoever; and the fact that the Government may have formulated, furnished, or in any way supplied the said drawings, specifications, or other data is not to be regarded by implication or otherwise as in any manner licensing the holder or any other person or corporation, or conveying any rights or permission to manufacture, use or sell any patented invention that may in any way be related thereto.

63-5-2
Report No. 9

Quarterly Progress Report No. III | December 1, 1962 to February 28, 1963

SOLID PROPELLANT MECHANICAL PROPERTIES INVESTIGATIONS

Prepared for:

ROCKET PROPULSION LABORATORIES
AIR FORCE SYSTEMS COMMAND
EDWARDS, CALIFORNIA

CONTRACT NO. AF 04(611)-8388

401 219

STANFORD RESEARCH INSTITUTE

Menlo Park, California

*SRI



**Best
Available
Copy**



March 25, 1963

Report No. 9

Quarterly Progress Report No. III | December 1, 1962 to February 28, 1963

SOLID PROPELLANT MECHANICAL PROPERTIES INVESTIGATIONS

Prepared for:

ROCKET PROPULSION LABORATORIES
AIR FORCE SYSTEMS COMMAND
EDWARDS, CALIFORNIA

CONTRACT NO. AF 04(611)-8388

By: Norman Fishman James A. Rinde

SRI Project No. PRU-4142

Approved:

THOR L. SMITH, DIRECTOR
PROPULSION SCIENCES DIVISION

Copy No.19

CONTENTS

LIST OF ILLUSTRATIONS	iii
I INTRODUCTION	1
II SUMMARY	2
III EXPERIMENTAL PROGRAM AND RESULTS	3
A. Constant Strain	3
B. Constant Strain Rate	3
C. Constant Load	6
D. Constant Loading Rate	8
E. Dilatometric Studies	17
1. Apparatus	17
2. Constant Load.	17
3. Constant Strain	18
4. Constant Strain Rate	22
F. Glass Temperature	24
IV FUTURE WORK	26
ACKNOWLEDGMENTS	26

ILLUSTRATIONS

Fig. 1	Failure Envelope ($\sigma_m - \epsilon_m$) for AEBA-15, Batch No. NF9/245	4
Fig. 2	Failure Envelope ($\sigma_b - \epsilon_b$) for AEBA-15, Batch No. NF9/245	5
Fig. 3	Comparison of Constant Load and Constant Loading Rate Rupture Data with Failure Envelopes for AEBA-15	7
Fig. 4	Constant Load Results for AEBA-15, Batch No. NF9/245, Tested at 100°F	9
Fig. 5	Constant Load Results for AEBA-15, Batch No. NF9/245, Tested at 40°F	10
Fig. 6	Constant Load Results for AFBA-1, Batch No. NF1/237, Tested at 100°F	11
Fig. 7	Constant Load Results for AFBA-1, Batch No. NF1/237, Tested at 40°F	12
Fig. 8	Strain-Time Relationships for AEBA-15, Batch No. NF9/245, Tested at Constant Loading Rate, 100°F	13
Fig. 9	Strain-Time Relationships for AEBA-15, Batch No. NF9/245, Tested at Constant Loading Rate, 40°F	14
Fig. 10	Strain-Time Relationships for AFBA-1, Batch No. NF1/237, Tested at Constant Loading Rate, 100°F	15
Fig. 11	Strain-Time Relationships for AFBA-1, Batch No. NF1/237, Tested at Constant Loading Rate, 40°F	16
Fig. 12	Volume Change and Strain as Functions of Time During a Constant Load Test of AFBA-1.	18
Fig. 13	Results of Constant Load to Constant Strain Test on AFBA-1, Batch No. NF3/239	19
Fig. 14	Results of Constant Strain Rate to Constant Strain Test on AFBA-1, Batch No. NF 3/239.	20
Fig. 15	Comparison of Volume Change Data from Constant Load and Constant Strain Rate Tests on AFBA-1, Batch No. NF3/239	21

ILLUSTRATIONS (Continued)

Fig. 16	Effects of Strain Rate on Volume Change: AFBA-1, Batch No. NF1/237, 100°F	22
Fig. 17	Effects of Strain Rate on Volume Change: AEBA-15, Batch No. NF9/245, 100°F	23
Fig. 18	Stress-Strain Curves for a Constant Strain Rate Test of AFBA-1 at 0.04 min ⁻¹ , 100°F	25

I INTRODUCTION

A detailed understanding of the mechanical behavior of solid propellants is required to advance the state-of-the-art of solid rocket technology. Knowledge of failure mechanisms and establishment of failure criteria are necessary before methods of stress analysis can become useful in describing and predicting solid grain malfunction.

In this research program we are investigating in detail the large deformation behavior and ultimate properties of solid propellants by means of uniaxial tension tests under conditions of constant strain rate, constant load, constant loading rate, and constant strain. In addition to the conventional test methods, attendant volume changes are being determined under selected conditions by performing the test in a specially constructed dilatometer. Particular emphasis is being placed on the contribution made by the binder-oxidant interfacial region to the mechanical behavior of solid propellants. The general objective of the research is to relate mechanical behavior and failure mechanisms to propellant microstructure.

This is the third Quarterly Progress Report of our investigations under Contract No. AF 04(611)-8388, with Lt. Frank N. Kelley, Rocket Propulsion Laboratories, Edwards Air Force Base, as project officer. The period covered by this report is December 1, 1962, to February 28, 1963.

II SUMMARY

Mechanical properties (consisting of results from constant strain rate, constant load, and constant loading rate tests) of the two compositions AFBA-1 and AEBA-15 have been determined. Volume change data are being obtained by performing selected tests in the dilatometer. All work thus far has been with desiccated specimens tested under dry conditions.

Dilatometric tests under conditions of constant load have verified the thesis that the linear strain-time portion of the creep curve represents a region where dewetting is the process which controls the creep rate. In this region, the volume was found to increase linearly with time.

Constant strain tests in the dilatometer at 100°F showed that little or no volume change occurred after the selected value of constant strain was reached. Further, it was found that the physical state of a propellant was not dependent solely on strain but was also a function of path. When comparable extension rates under constant load and constant strain rate conditions were used to extend the specimens to selected values of constant strain, it was found that different volume changes resulted, the higher volume change being associated with extension under constant load.

Volume change measurements during constant strain rate tests at 100°F showed that the volume change at large deformations increased with the strain rate, and further, that the minimum value of Poisson's ratio at large deformations decreased as the strain rate increased.

III EXPERIMENTAL PROGRAM AND RESULTS

Characterization of the mechanical properties of desiccated specimens of AFBA-1 (carboxy-terminated polybutadiene) and AEBA-15 (polyurethane) propellant compositions under conditions of constant strain rate, constant load, and constant loading rate has been largely completed. Dilatometric studies are in progress. Results are reported in such form as to enable inferences to be made and to provide descriptions of system behavior. Where possible, conclusions based on current data are also presented.

A. Constant Strain

Tests are being conducted to determine time-to-rupture as a function of strain for specimens of AEBA-15 and AFBA-1. These tests are being carried out with desiccated specimens under dry conditions at ambient temperature. Special constant strain racks have been fabricated to fit into laboratory storage facilities so that long time tests can be undertaken. Short time rupture data will be obtained both in the creep apparatus and in the dilatometer.

B. Constant Strain Rate

Results of constant strain rate tests of AFBA-1 were presented in our Quarterly Progress Report No. II. These were shown as failure envelopes representing rupture under various conditions of strain rate and temperature. Failure envelopes for AEBA-15, Batch NF 9/245, are shown in Figs. 1 and 2; data were obtained at two strain rates, 4.0 and 0.04 min^{-1} , and at six temperatures between 0 and 160°F.

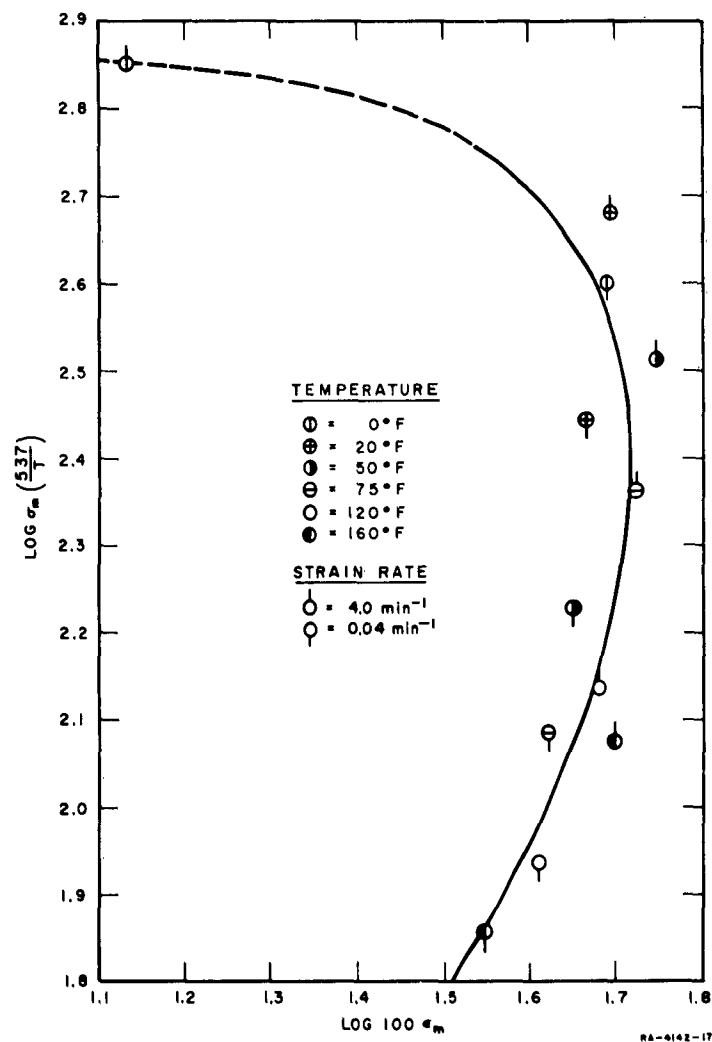


FIG. 1 FAILURE ENVELOPE ($\sigma_m - \epsilon_m$) FOR AEBA-15, BATCH NO. NF9/245

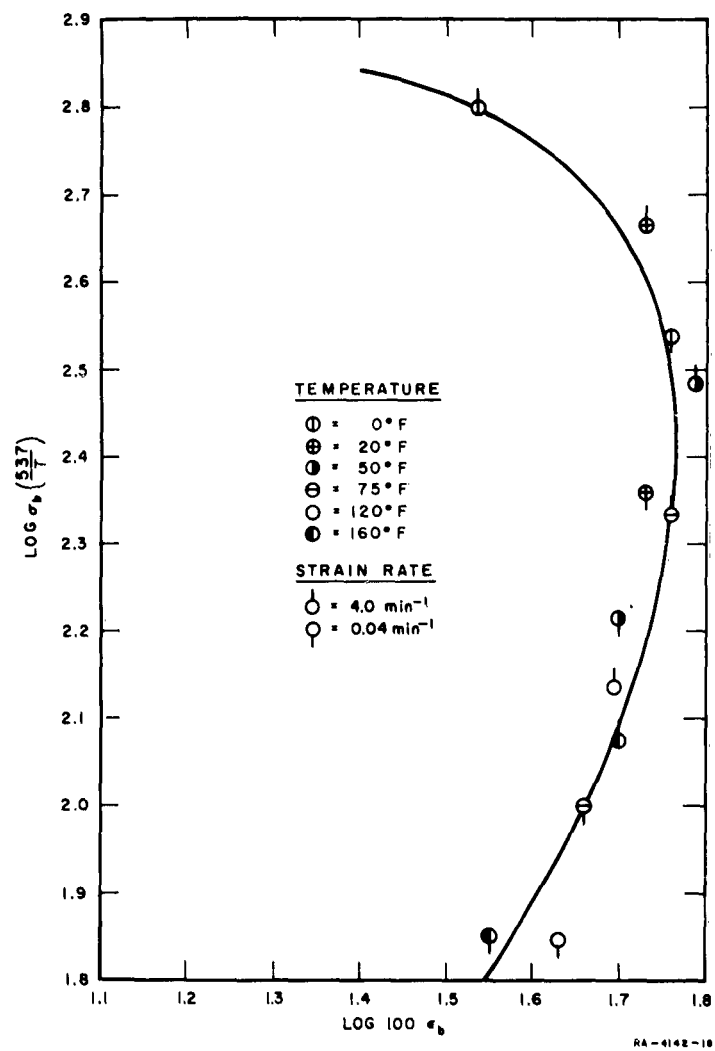


FIG. 2 FAILURE ENVELOPE ($\sigma_b - \epsilon_b$) FOR AEBA-15,
BATCH NO. NF9/245

The failure envelopes for AEBA-15, similar to those for AFBA-1, show a relatively large range of stress over which values of strain at maximum stress and strain at rupture are sensibly constant. Actual failure properties of the two compositions differ considerably, the better properties (i.e., greater stresses and strains) being associated with AEBA-15. In both cases, best properties are obtained in the temperature range of 50 to 75°F. The table below presents comparative data for the two compositions.

Maximum Properties (approx.)	AFBA-1	AEBA-15
ϵ_m , in./in.	0.45	0.51
σ_m , psi	100-185	200-315
ϵ_b , in./in.	0.52	0.57
σ_b , psi	100-185	225-315

Figure 3 shows rupture data from constant load and constant loading rate tests (which are presented later in this report) superimposed on the failure envelopes. Though rupture appeared to occur at somewhat greater strains, agreement with the failure envelopes was sufficiently good to indicate only a small effect of method of straining on ultimate properties. A similar representation for AFBA-1 (constant load data only) was shown in Fig. 7 of Quarterly Progress Report No. II.

C. Constant Load

Constant load tests of AEBA-15 and AFBA-1 were made at two temperatures and several loads to characterize further their mechanical behavior. In general, their behavior is typical of other propellants in that the strain-time relationship shows at first a region like that expected for viscoelastic materials. This is followed by another region in which the strain increases linearly with time and in which the dewetting process is rate-controlling; the third and final region is that in which failure occurs. Results are shown in Figs. 4-7 as log compliance vs. log time. Tests of AFBA-1, reported in Quarterly Progress Report No. II, were repeated with another batch, NF 1/237. All specimens were desiccated and bagged to insure dry conditions during the time of the test.

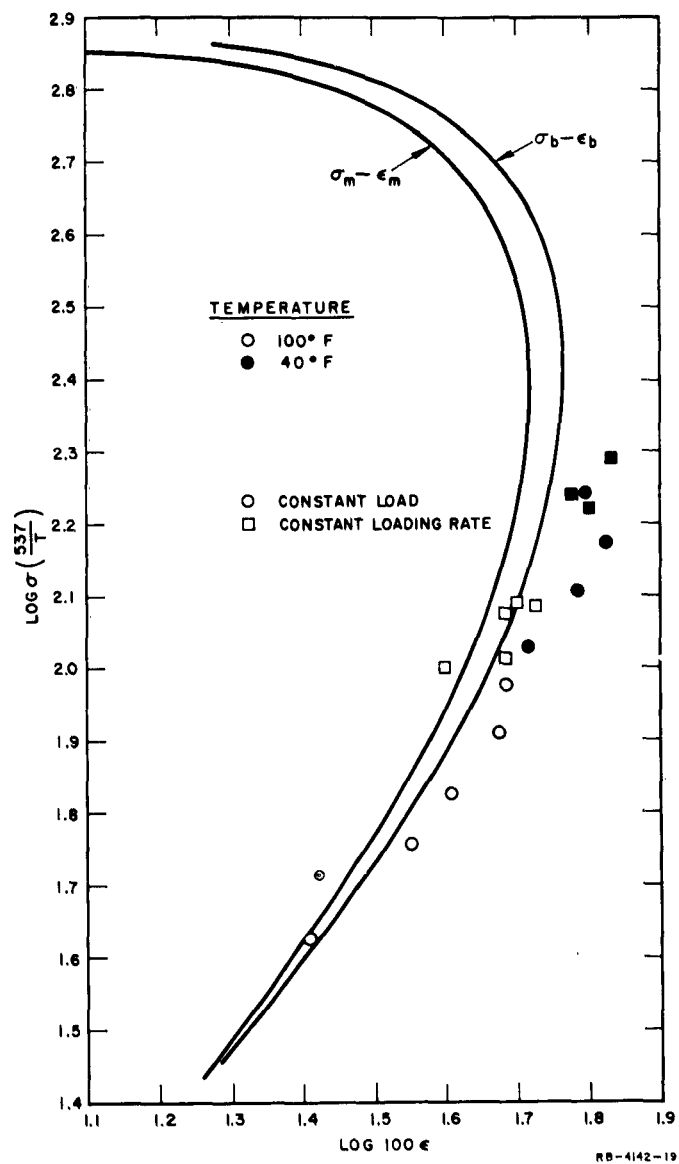


FIG. 3 COMPARISON OF CONSTANT LOAD AND CONSTANT LOADING RATE RUPTURE DATA WITH FAILURE ENVELOPES FOR AEBA-15

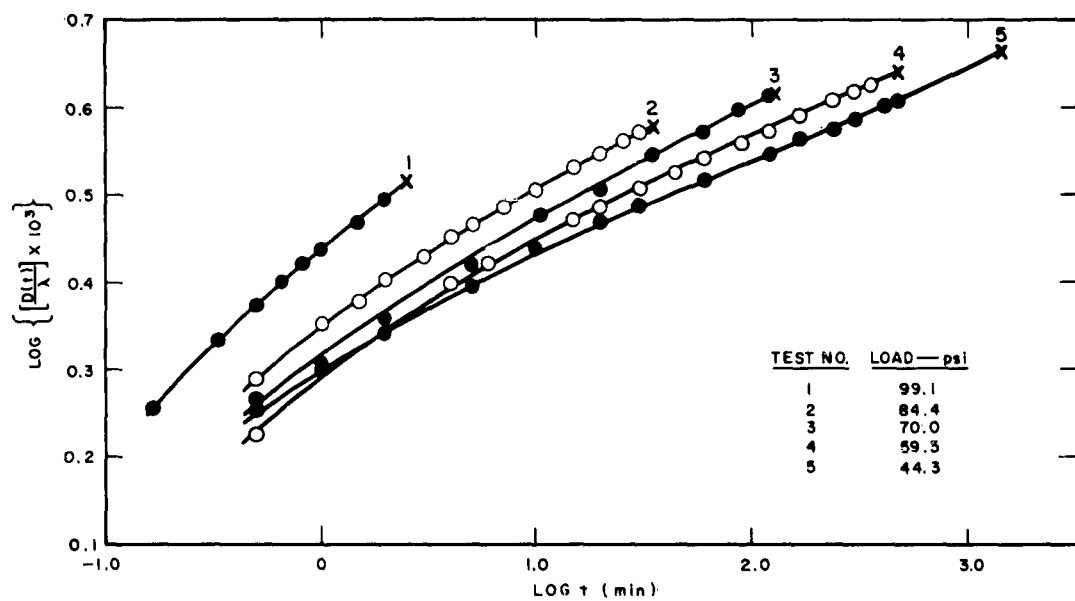
In examining the curves of Figs. 4 and 5, which present data for AEBA-15, we can note the following points: (1) the compliance at break at different loads decreases approximately linearly with increasing load, thus yielding a basis for estimating the time to failure at a given stress, (2) values of compliance are generally lower than those determined for specimens equilibrated at ambient humidity, (3) the curves do not appear to have a common value of compliance at low strains and short times, indicating dependence of compliance on load, and (4) data at 40°F differ in that the curves bend downward, as if representative of transition zone behavior, and tend toward load independence at high strains near rupture.

The data for AFBA-1, shown in Figs. 6 and 7, are similar to those for AEBA-15 except that behavior at 40°F is similar to that at 100°F. Perhaps the greatest difference between compositions is the deviation from the straight line relationship which occurs just prior to rupture of the AFBA-1 specimens. This type of behavior is normal for humidified materials; since it also occurs in the desiccated AFBA-1 but not in the desiccated AEBA-15, the failure mechanisms of the two compositions may be quite different. It appears also that extrapolation of AFBA-1 data to short times tends toward a common compliance.

D. Constant Loading Rate

Data from constant loading rate tests of AEBA-15 and AFBA-1 are presented as log strain vs. log time in Figs. 8-11. The tests were carried out at 40°F and 100°F over a range of loading rates limited by the test apparatus.

The data from these tests appear to be consistent and potentially useful for correlation with results of other tests. The two compositions appear to be similar in behavior as shown by the shape of the strain-time curves and by the apparent independence of strain at break on loading rate at a given temperature. As shown in Fig. 3, rupture strains are consistent with the failure envelope from constant strain rate data. For AEBA-15, Figs. 8 and 9, values for the average strain at break at 40°F and 100°F are 0.49 and 0.63, respectively.



RA-4142-20

FIG. 4 CONSTANT LOAD RESULTS FOR AEBA-15, BATCH NO. NF9/245, TESTED AT 100°F

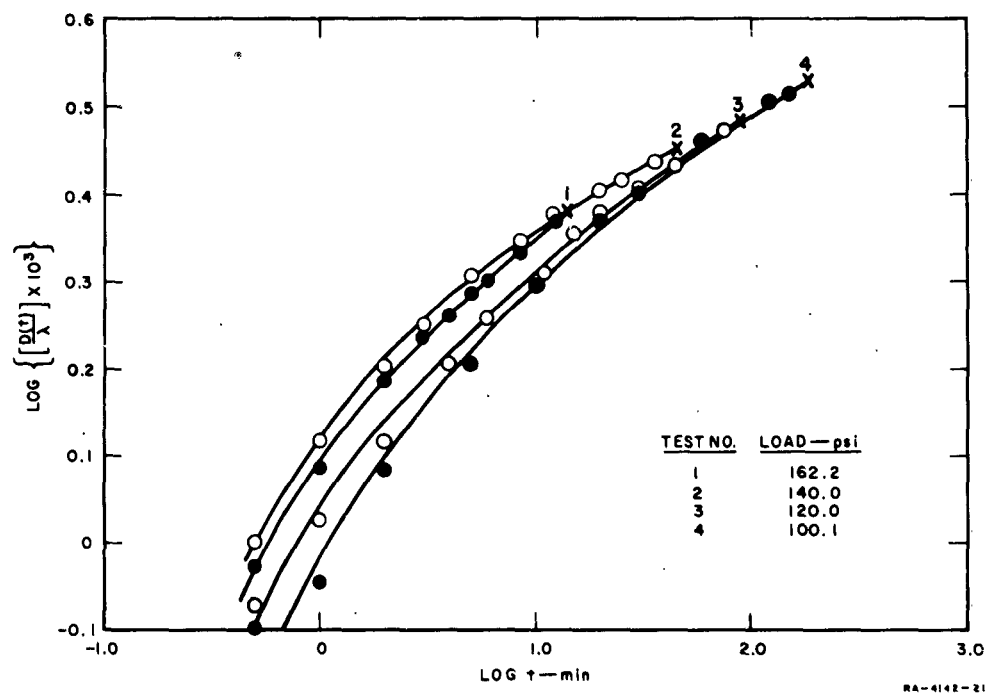


FIG. 5 CONSTANT LOAD RESULTS FOR AEBA-15, BATCH NO. NF9/245, TESTED AT 40°F

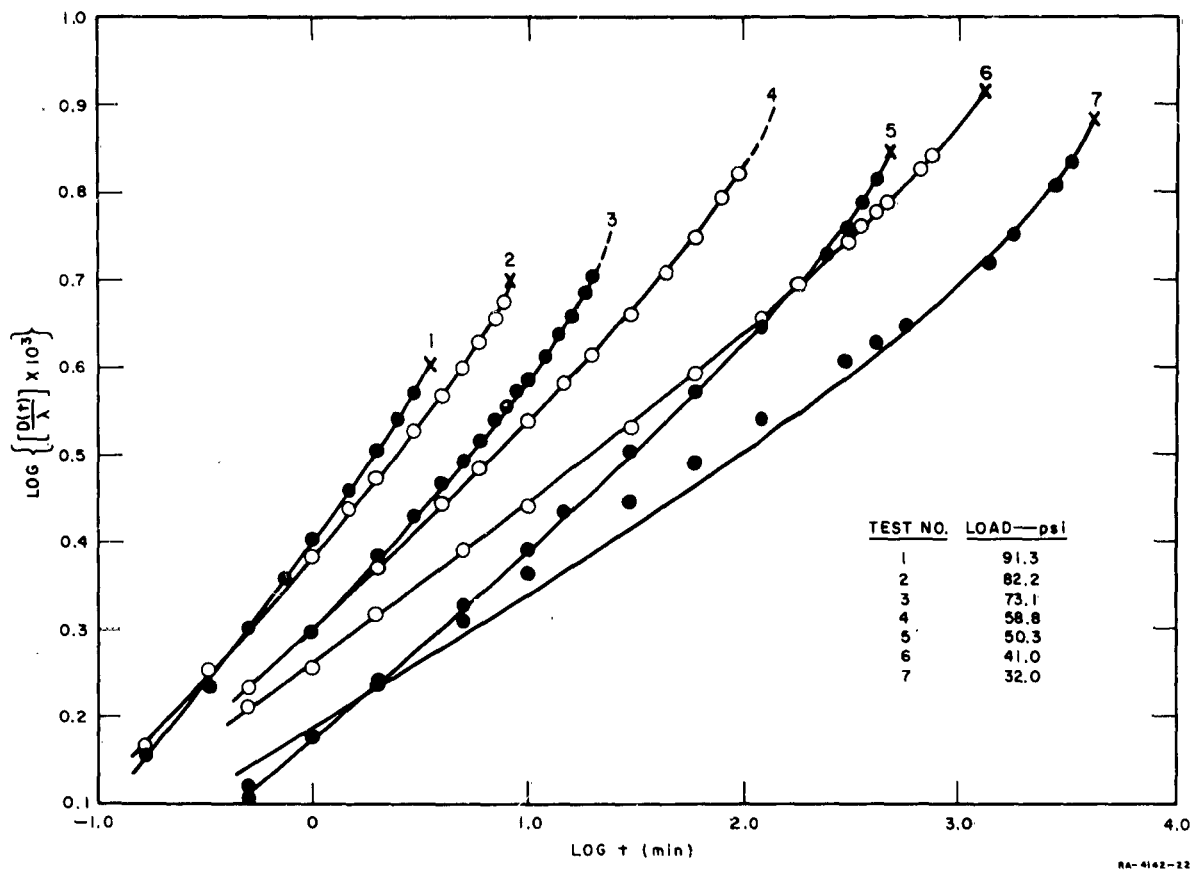


FIG. 6 CONSTANT LOAD RESULTS FOR AFBA-1, BATCH NO. NF1/237, TESTED AT 100°F

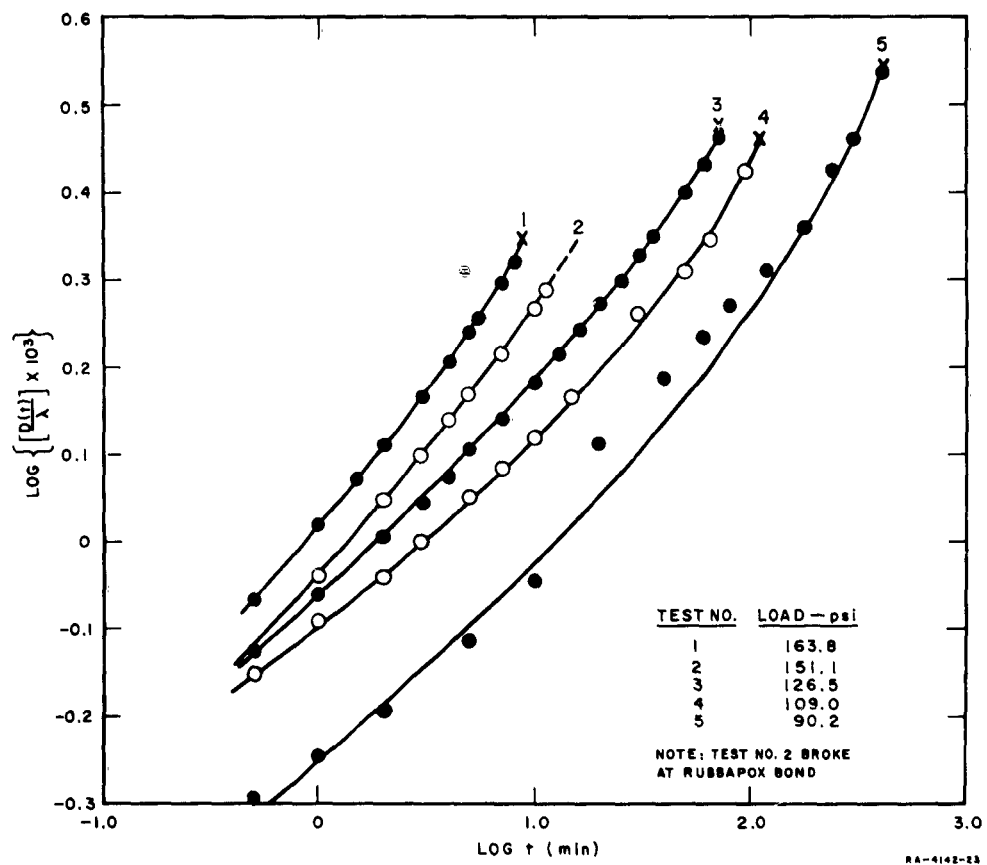


FIG. 7 CONSTANT LOAD RESULTS FOR AFBA-1, BATCH NO. NF1/237, TESTED AT 40°F

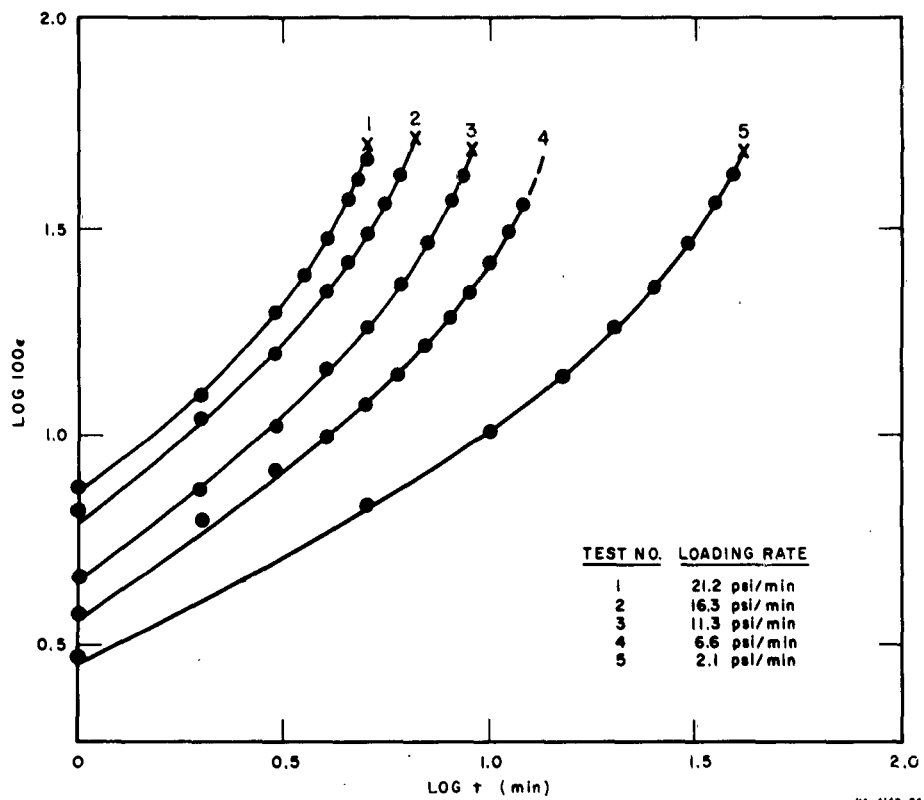


FIG. 8 STRAIN-TIME RELATIONSHIPS FOR AEBA-15, BATCH NO. NF9/245, TESTED AT CONSTANT LOADING RATE, 100°F

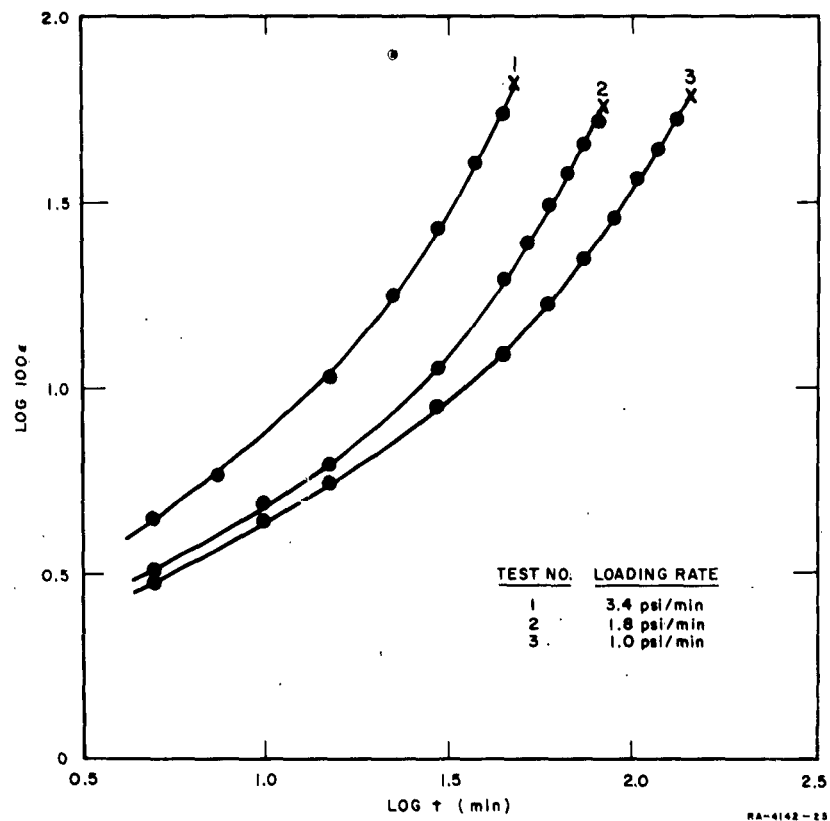


FIG. 9 STRAIN-TIME RELATIONSHIPS FOR AEBA-15, BATCH NO. NF9/245, TESTED AT CONSTANT LOADING RATE, 40°F

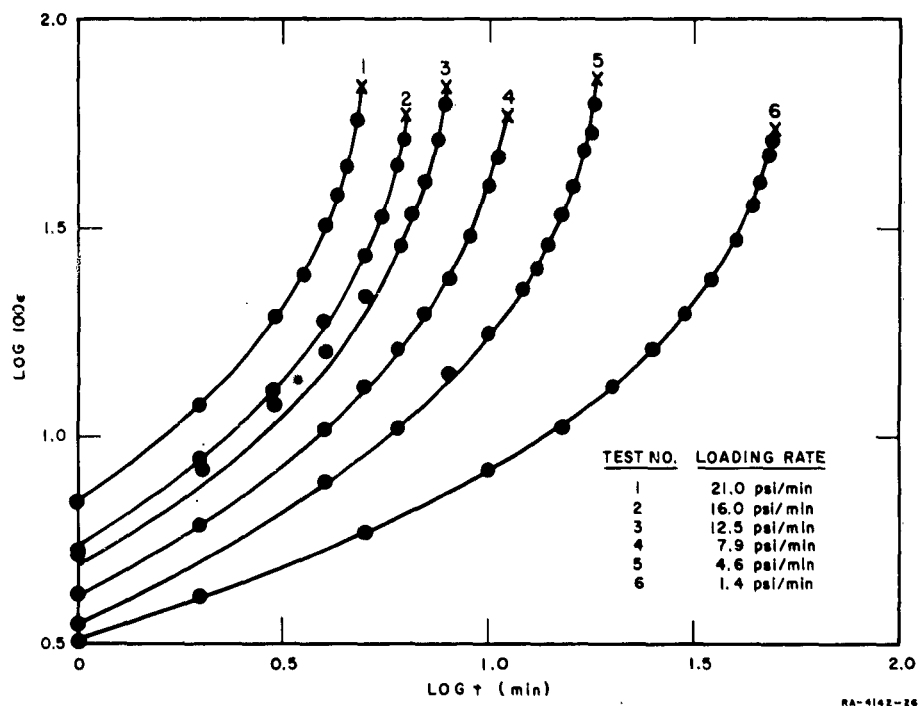


FIG. 10 STRAIN-TIME RELATIONSHIPS FOR AFBA-1, BATCH NO. NF1/237, TESTED AT CONSTANT LOADING RATE, 100°F

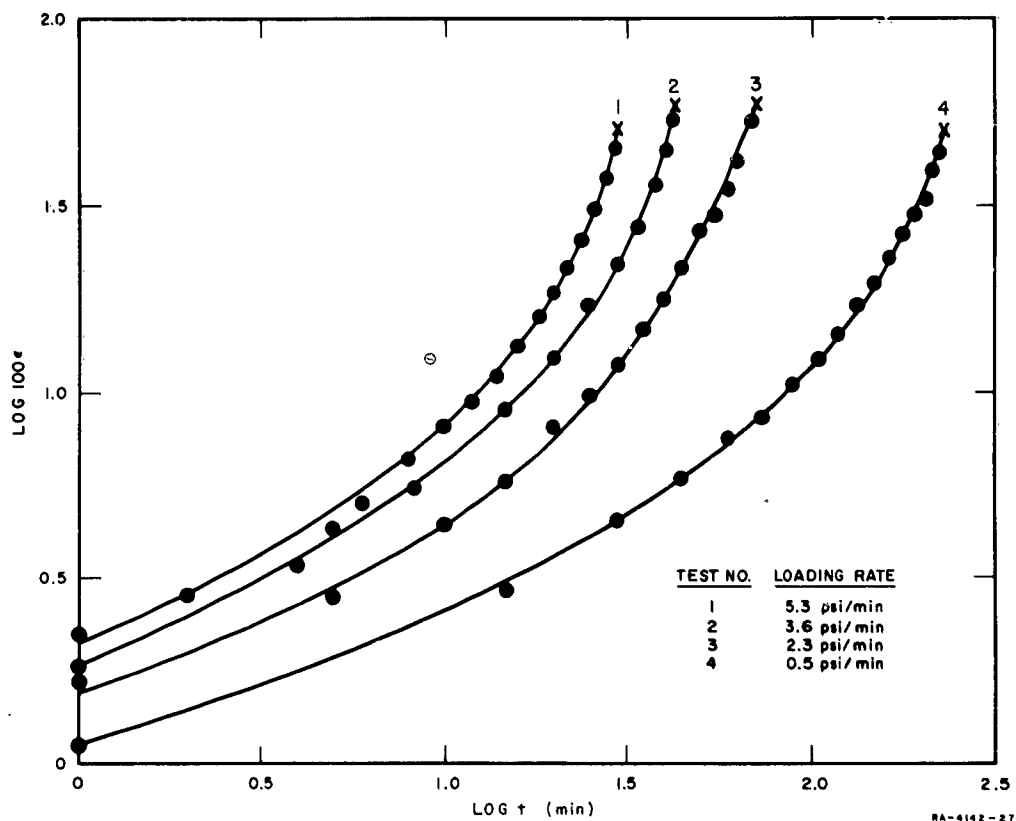


FIG. 11 STRAIN-TIME RELATIONSHIPS FOR AFBA-1, BATCH NO. NF1/237, TESTED AT CONSTANT LOADING RATE, 40°F

E. Dilatation

1. Apparatus

The dilatometer is operating well and tests are being run on almost a routine basis. However, some difficulties still remain to be resolved. Some loss of pressure is noted over long periods of time due either to minor leaks in the system or to a minor leak in the bellows of the transducer. Tests which involve two hours or less are not seriously affected, but longer term tests are not possible until the deficiency is corrected. Another problem, not unique to the dilatometer, is in undertaking high load creep tests without breaking the bond at the tab; a "softer" application of the load should improve this situation. Another problem associated with creep testing has been encountered in attempting creep recovery experiments. Before this type of experiment can be run we will have to investigate other methods of counterbalancing loads and/or the use of a more powerful servo motor.

2. Constant Load

A typical volume change curve obtained during a constant load experiment is shown in Fig. 12. These data show the parallelism between the normal strain-time and the volume change-time curves, and serve to verify the thesis that the linear strain-time portion of creep behavior is in a region where the dewetting process is the controlling mechanism. Further verification will be sought (1) by performing these experiments at different temperatures to determine if "activation energies" for the straining and the volume change processes are the same,⁹ and (2) by determining if the load dependencies of the two processes are the same.

If possible, creep recovery data at several temperatures will also be obtained in the dilatometer to determine if activation energies for the rewetting process and for strain recovery are the same. With such data, a measure of the energy of the particle-binder bond might be obtained as the difference between the activation energies for the dewetting and rewetting processes.

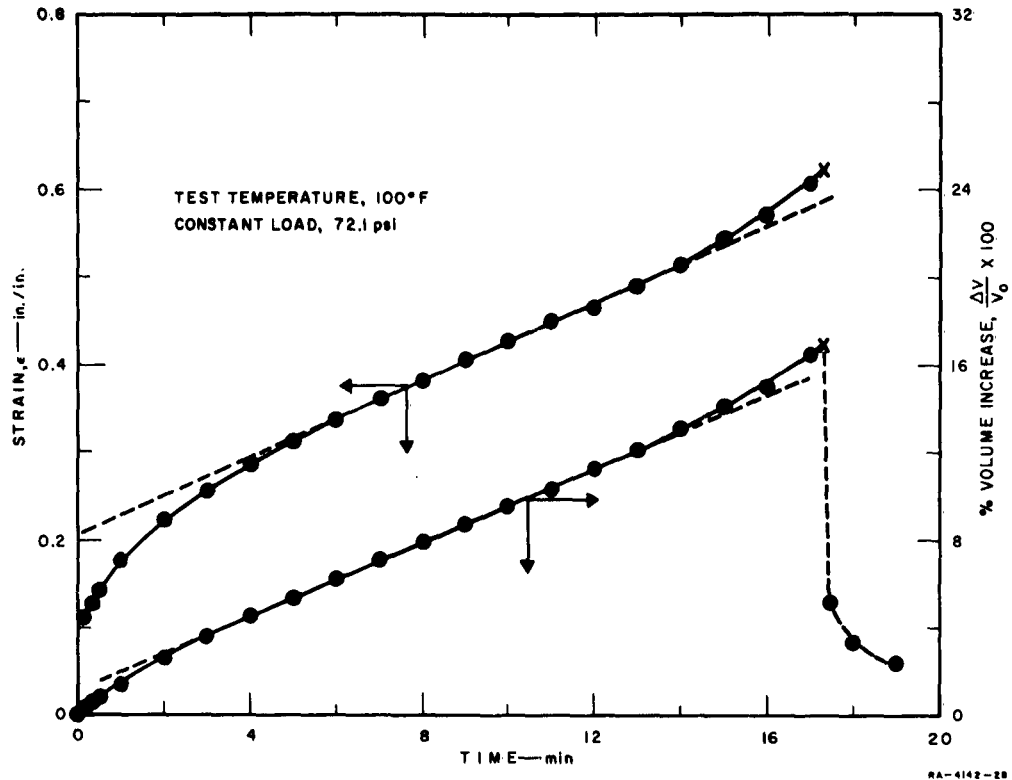


FIG. 12 VOLUME CHANGE AND STRAIN AS FUNCTIONS OF TIME DURING A CONSTANT LOAD TEST OF AFBA-1

3. Constant Strain

Studies of constant strain behavior were undertaken by extending the specimen to a fixed value of strain and observing the volume change during the extension process and after the desired value of constant strain had been reached. Results of two such tests are shown in Figs. 13 and 14; in both cases the value of constant strain was 0.35. Extension under constant load (Fig. 13) and extension at a constant strain rate (Fig. 14) were conducted so that the desired value of strain was achieved in approximately the same time, thus providing comparability of extension rates. In both cases, little or no volume change was noted after the strain was held constant.

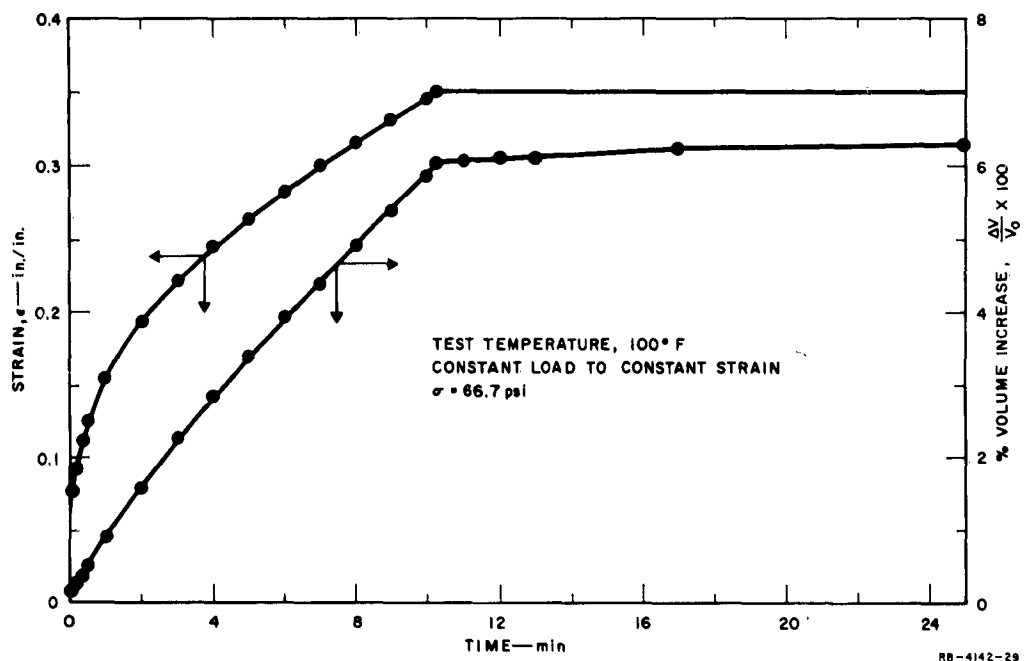


FIG. 13 RESULTS OF CONSTANT LOAD TO CONSTANT STRAIN TEST ON AFBA-1, BATCH NO. NF3/239

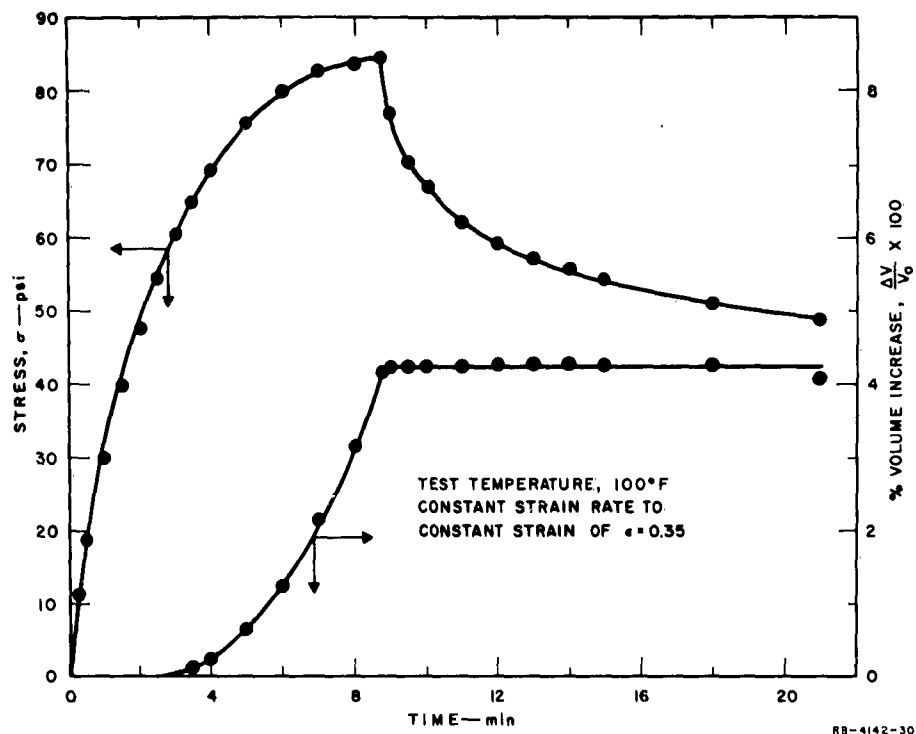


FIG. 14 RESULTS OF CONSTANT STRAIN RATE TO CONSTANT STRAIN TEST ON AFBA-1, BATCH NO. NF3/239

Two interesting observations can be made from these data. First, the physical state of a propellant at a fixed value of strain is not independent of path, as demonstrated by the 6% and 4% volume changes recorded for the constant load and constant strain rate tests, respectively. The other point of interest is that the expected stress relaxation occurs with no attendant change in volume. We can hypothesize at this time that such behavior may be due to (1) a stress-averaging process which rearranges wetted and dewetted regions yet does not affect the net volume, or to (2) a particle-particle rearrangement in which individual particles shift to relieve stresses without affecting volumes of the individual vacuoles.

The data from these tests were also plotted in Fig. 15 as log volume versus log extension ratio to arrive at instantaneous values of Poisson's ratio as a function of extension ratio. We observe that in either case little or no volume change occurs until a strain of about 0.10 is reached. Then as strain increases, the volume change at constant load increases more rapidly than that at constant strain rate, until a constant slope is achieved. Values of Poisson's ratio shown in Fig. 15 (0.3) appear to be the same for each test at high strain levels.

These observations lead to an anomaly. Since no volume change occurs after the strain is fixed, then one might assume that the extent of dewetting was dependent upon strain only. Yet one notes that different volumes, and hence different degrees of dewetting, result when different paths are taken to the same value of strain. A major objective of analyses of results, as more tests are undertaken, is to determine the relationship between path (i. e., stress-strain-time) and the dewetting process.

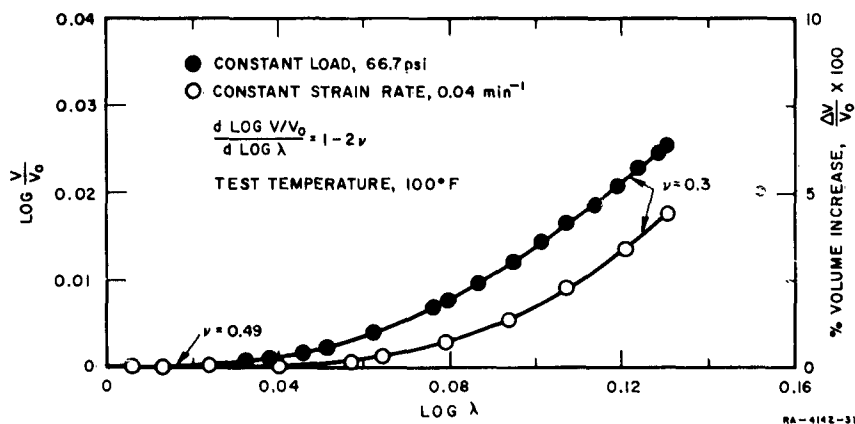


FIG. 15 COMPARISON OF VOLUME CHANGE DATA FROM CONSTANT LOAD AND CONSTANT STRAIN RATE TESTS ON AFBA-1, BATCH NO. NF3/239

4. Constant Strain Rate

Constant strain rate tests were conducted on both AEBA-15 and AFBA-1 at 100°F and at three strain rates. The results of these tests are shown in Figs. 16 and 17 as plots of log volume vs. log extension ratio. In all cases, little or no volume change was noted at strains below about 0.10; at larger strains, the rate of volume increase and the volume at rupture increased with the strain rate. Minimum values of Poisson's ratio, (at large strains where log volume change is linearly proportional to log extension ratio) also appear to be dependent on strain rate; lower values of ν are achieved at higher strain rates. Again, these data illustrate the dependence of dewetting upon path; further work designed to establish firm relationships between strain rate and dewetting will aid in establishing the stress-strain-time dependency of the dewetting process.

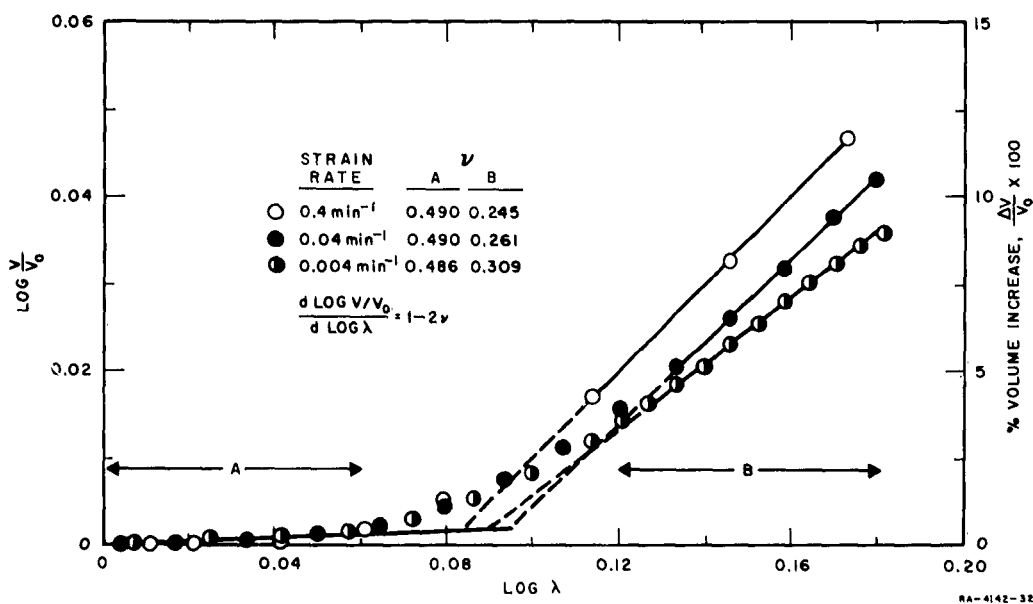


FIG. 16 EFFECTS OF STRAIN RATE ON VOLUME CHANGE: AFBA-1, BATCH NO. NF1/237, 100°F

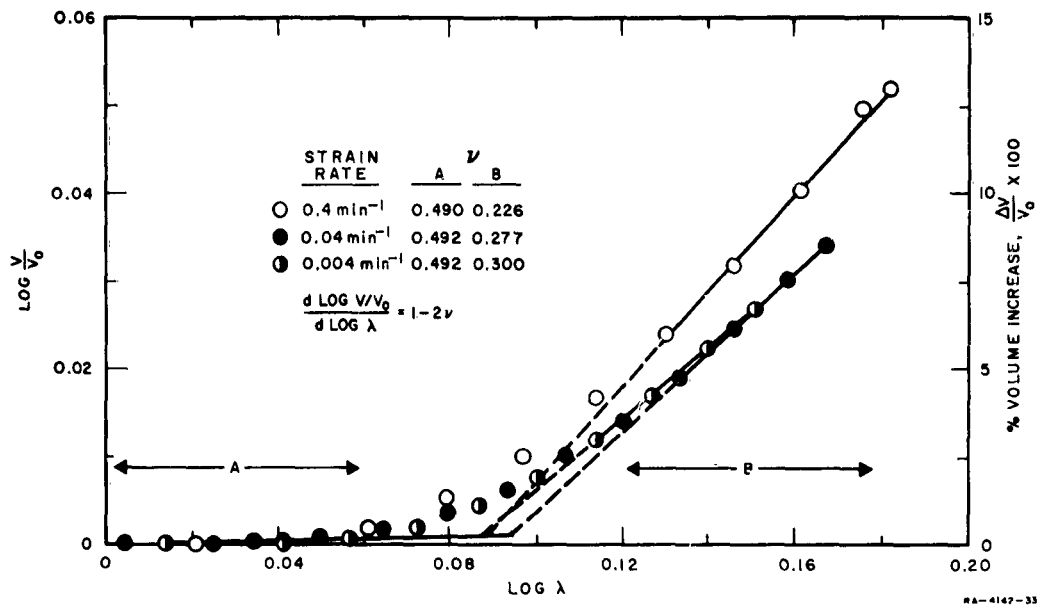


FIG. 17 EFFECTS OF STRAIN RATE ON VOLUME CHANGE: AEBA-15, BATCH NO. NF9/245, 100°F

A method of analysis is employed on another program at Stanford Research Institute* which defines a strain-independent constant strain rate modulus,

$$F(t) = \frac{g(\epsilon)\sigma}{\epsilon}$$

where,

σ is the stress which depends on strain and time

ϵ is the strain

$g(\epsilon)$ is a function only of strain.

*Smith, T.L., and Smith, J.R., Quarterly Technical Summary Report No. 5, SRI Project No. PRU-3739, Contract No. NOW-61-1057-d, ARPA Order No. 22-61, October 31, 1962.

For values of strain up to about 0.10, $g(\epsilon)$ was found to be equal to λ . At larger strains, the data were relatively well represented by $g(\epsilon) = \lambda^2$, although values of $F(t)$ at various temperatures were different than for strains less than 0.1. In examining our data, we found that if λ were raised to the power, $3-4\nu$, the function $g(\epsilon)$ found by Smith was well duplicated. Figure 18 shows a conventional stress strain curve and its counterpart $g(\epsilon)\sigma$ vs. ϵ , where $g(\epsilon) = \lambda^{3-4\nu}$. Though this function of strain may not fit the criterion of temperature and time independence, the general approach appears to be promising as a means of interrelating test data and developing a relationship between path (i. e., stress-strain-time) and the dewetting process.

F. Glass Temperature

Glass temperatures (T_g) for the two compositions being studied were determined with an air dilatometer; values of -62°C for AFBA-1 and -39°C for AEBA-15 were found. The glass temperature of another composition, AEBA-10, was determined with an air dilatometer and by hydrostatic weighing in iso octane; measured values of T_g were -61°C and -48°C , respectively.

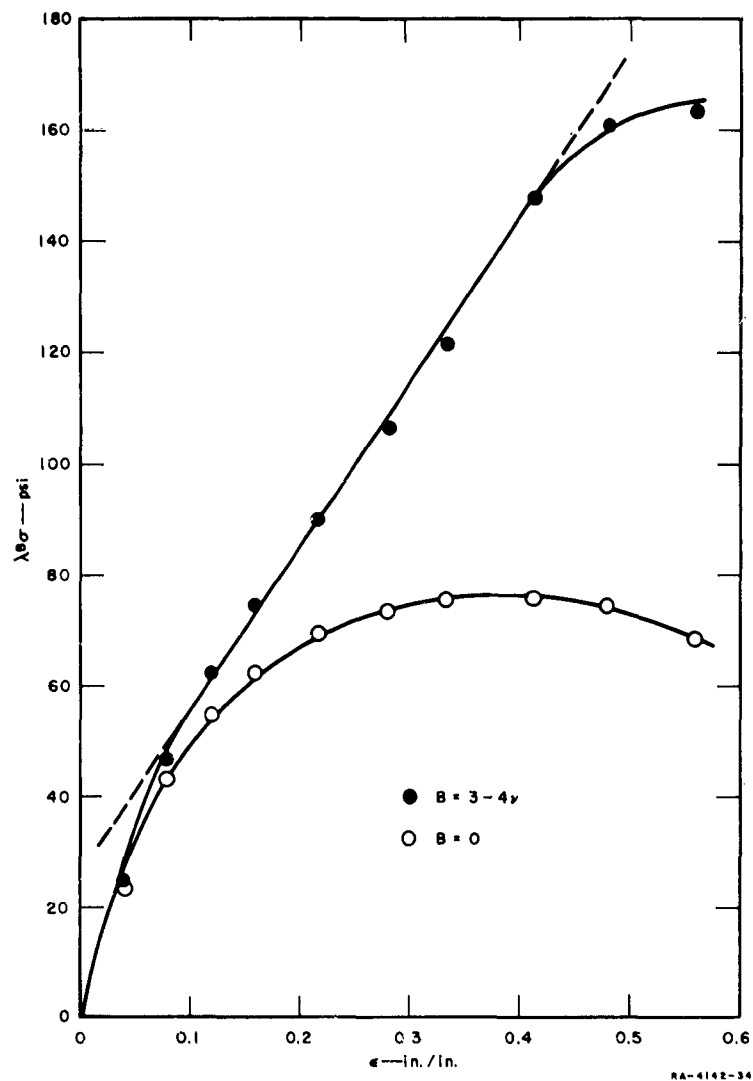


FIG. 18 STRESS-STRAIN CURVES FOR A CONSTANT STRAIN RATE TEST OF AFBA-1 AT 0.04 min^{-1} , 100°F

IV FUTURE WORK

The major portion of the work planned involves tests using the dilatometer. These include (1) further constant strain rate tests at several rates and temperatures, (2) additional constant load tests at several loads and temperatures, including creep recovery, if possible, and (3) constant strain tests to investigate the effects of the temperature and the influence of path of extension.

Additional experimental work includes completion of the constant strain time-to-break studies, and duplication of many of the tests under conditions of 20 and 42% relative humidity. Data analysis and development of hypotheses as to mechanisms of mechanical behavior will be continued.

ACKNOWLEDGMENTS

Suggestions for analysis of data were made by Dr. Thor L. Smith, and assistance in conducting the experimental program was provided by Edward A. Hillam.

Norman Fishman

Norman Fishman, Manager
Propellant Evaluation Section

James A. Rinde

James A. Rinde, Chemist

**STANFORD
RESEARCH
INSTITUTE**

**MENLO PARK
CALIFORNIA**

Regional Offices and Laboratories

Southern California Laboratories
820 Mission Street
South Pasadena, California

Washington Office
808 17th Street, N.W.
Washington 5, D.C.

New York Office
270 Park Avenue, Room 1770
New York 17, New York

Detroit Office
The Stevens Building
1025 East Maple Road
Birmingham, Michigan

European Office
Pelikanstrasse 37
Zurich 1, Switzerland

Japan Office
911 Iino Building
22, 2-chome, Uchisaiwai-cho, Chiyoda-ku
Tokyo, Japan

Representatives

Honolulu, Hawaii
Finance Factors Building
195 South King Street
Honolulu, Hawaii

London, England
19 Upper Brook Street
London, W. 1, England

Milan, Italy
Via Macedonio Melloni 40
Milano, Italy

London, Ontario, Canada
P.O. Box 782
London, Ontario, Canada